Elsevier Editorial System(tm) for Developmental Biology
Manuscript Draft

Manuscript Number:

Title: VEGF Signals Induce Trailblazer Cell Identity that Drives Neural Crest Migration

Article Type: Full Length Article

Section/Category: Developmental Biology - Main

Keywords: Neural crest
Chick
Cell migration
Embryonic microenvironment
gene expression
molecular profile
computational modeling
trailblazers

Corresponding Author: Dr. Paul Kulesa,

Corresponding Author's Institution: Stowers Institute for Medical Research

First Author: Rebecca McLennan, PhD

Order of Authors: Rebecca McLennan, PhD; Linus J Schumacher; Jason A Morrison; Jessica M Teddy; Dennis A Ridenour; Andrew C Box; Craig L Semerad; Hua Li; William McDowell; David Kay; Philip K Maini; Ruth E Baker; Paul Kulesa

Abstract: Embryonic neural crest cells travel in discrete streams to precise locations throughout the head and body. We previously showed that cranial neural crest cells respond chemotactically to vascular endothelial growth factor (VEGF) and that cells within the migratory front have distinct behaviors and gene expression. We proposed a cell-induced gradient model in which lead neural crest cells read out directional information from a chemoattractant profile and instruct trailers to follow. In this study, we show that migrating chick neural crest cells do not display distinct lead and trailer gene expression profiles in culture. However, exposure to VEGF in vitro results in the upregulation of a small subset of genes associated with an in vivo lead cell signature. Timed addition and removal of VEGF in culture showed the neural crest cell gene expression changes were rapid. A computational model incorporating an integrate-and-switch mechanism for switching between cellular phenotypes predicted migration efficiency is influenced by behavior switching. Tissue transplantations that presented ectopic sources of VEGF to the trailer neural crest cell subpopulation showed diverted cell trajectories and stream alterations consistent with model predictions. Gene profiling revealed upregulation of a subset of 'lead' genes in diverted cells that encountered the VEGF. Injection of Np1-Fc into the trailer subpopulation or electroporation of VEGF morpholino to reduce VEGF signaling failed to alter trailer neural crest cell trajectories, suggesting trailers do not require VEGF to maintain coordinated migration. These results indicate that VEGF is one of the signals that establishes lead cell identity and its chemoattractant profile is critical to neural crest cell migration.

Suggested Reviewers: Philippe Soriano PhD
Professor, Developmental and Regenerative Biology, Mount Sinai Hospital
philippe.soriano@mssm.edu

Jeffrey Bush PhD
Assistant Professor, Cell and Tissue Biology, University of California
Jeffrey.Bush@ucsf.edu

Laura Gammill PhD
Associate Professor, College of Biological Sciences, University of Minnesota
gammi001@umn.edu

Rodney Stewart PhD
Assistant Professor, Oncological Sciences, University of Utah
rodney.stewart@hci.utah.edu

Lisa A Taneyhill PhD
Assistant Professor, Animal and Avian Sciences, University of Maryland
ltaney@umd.edu

Opposed Reviewers:

STOWERS INSTITUTE®
FOR MEDICAL RESEARCH

1 June, 2015

Professor Marianne Bronner
Editor-in-Chief, Developmental Biology
Albert Billings Ruddock Professor of Biology
California Institute of Technology
1200 E. California Blvd.
Pasadena, CA, 91125

Dear Professor Bronner,

On behalf of the authors of the enclosed manuscript entitled "**VEGF signals induce trailblazer cell identity that drives neural crest migration**", we are pleased to submit our work for publication consideration in Developmental Biology.

We previously showed that cranial neural crest cells respond chemotactically to vascular endothelial growth factor (VEGF) in vivo and postulated a cell-induced gradient model for migration. We recently identified a unique molecular signature associated with cranial neural crest cells narrowly confined to the migratory front which we termed, 'trailblazers', further supporting our model that lead cells readout VEGF directional signals and instruct trailers to follow. What remained unknown was whether VEGF is one of the microenvironmental signals that establish the trailblazer signature and its importance to direct the trajectories of all neural crest cells.

In this study, we show that migrating chick cranial neural crest cells do not display distinct lead and trailer gene expression profiles in culture. However, exposure to VEGF in vitro induces the expression of a small subset of trailblazer genes that are upregulated rapidly. Computer model simulations that incorporate an integrate-and-switch mechanism (to model a lead-to-trailer cell behavior) predict migration efficiency is influenced by behavior switching.

To test the importance of the VEGF chemoattractant profile, we placed VEGF-producing cells either within or adjacent to a typical cranial neural crest stream and show that cells divert trajectories and change gene expression to a trailblazer-like profile after responding to ectopic VEGF. Interestingly, loss of VEGF signals within the trailer neural crest subpopulation have little effect on cell trajectories. These data suggest that VEGF is one of the signals that induce trailblazer cell identity and support our model that trailer neural crest cells are instructed by leaders.

The results of this paper should be of interest to the development and cancer biology communities because it provides critical information about the importance of VEGF to direct cell movements and gene expression, processes fundamental in both development and cancer.

Best wishes,

Paul M. Kulesa, PhD
Professor and Director of Imaging/KulesaLab
Stowers Institute for Medical Research
Kansas City, MO 64110

VEGF Signals Induce Trailblazer Cell Identity that Drives Neural Crest Migration

by Rebecca McLennan[1*], Linus J. Schumacher[2*], Jason A. Morrison[1], Jessica M. Teddy[1], Dennis A. Ridenour[1], Andrew C. Box[1], Craig L. Semerad[1], Hua Li[1], William McDowell[1], David Kay[2], Philip K. Maini[2], Ruth E. Baker[2], and Paul M. Kulesa[1,3**]

1 Stowers Institute for Medical Research, 1000 E. 50th St, Kansas City, MO, 64110, USA

2 University of Oxford, Wolfson Centre for Mathematical Biology, Mathematical Institute, Andrew Wiles Building, Radcliffe Observatory Quarter, Woodstock Road, Oxford, OX2 6GG, UK

3 Department of Anatomy and Cell Biology, University of Kansas School of Medicine, Kansas City, KS, 66160, USA

*both authors contributed equally to this work, **corresponding author

Abstract

Embryonic neural crest cells travel in discrete streams to precise locations throughout the head and body. We previously showed that cranial neural crest cells respond chemotactically to vascular endothelial growth factor (VEGF) and that cells within the migratory front have distinct behaviors and gene expression. We proposed a cell-induced gradient model in which lead neural crest cells read out directional information from a chemoattractant profile and instruct trailers to follow. In this study, we show that migrating chick neural crest cells do not display distinct lead and trailer gene expression profiles in culture. However, exposure to VEGF in vitro results in the upregulation of a small subset of genes associated with an in vivo lead cell signature. Timed addition and removal of VEGF in culture showed the neural crest cell gene expression changes were rapid. A computational model incorporating an integrate-and-switch mechanism for switching between cellular phenotypes predicted migration efficiency is influenced by behavior switching. Tissue transplantations that presented ectopic sources of VEGF to the trailer neural crest cell subpopulation showed diverted cell trajectories and stream alterations consistent with model predictions. Gene profiling revealed upregulation of a subset of 'lead' genes in diverted cells that encountered the VEGF. Injection of Np1-Fc into the trailer subpopulation or electroporation of VEGF morpholino to reduce VEGF signaling failed to alter trailer neural crest cell trajectories, suggesting trailers do not require VEGF to maintain coordinated migration. These results indicate that VEGF is one of the signals that establishes lead cell identity and its chemoattractant profile is critical to neural crest cell migration.

Introduction

One of the most striking examples of embryonic cell migration is the multipotent, highly invasive neural crest. Neural crest cells exit the dorsal neural tube in a rostral-to-caudal order and are sculpted into discrete streams that travel throughout the landscape of the developing vertebrate embryo (Theveneau and Mayor, 2012; Kulesa and McLennan, 2015). Neural crest migration distributes cells to nearly every major organ. As such, a large class of neural-crest-related congenital birth defects has been termed neurocristopathies (Cordero et al., 2011; McKeown et al., 2013; Butler-Tjaden and Trainor, 2013; Kulesa et al., 2013). Neurocristopathies may severely affect craniofacial, cardiovascular and autonomic nervous system function. In addition, neural-crest-derived melanoma and neuroblastoma can be very aggressive cancers (Kulesa et al., 2013; Maguire et al., 2015). Thus, the invasive ability and significant contribution to organogenesis of the neural crest make this cell population an important model of study in development and cancer.

Advances in time-lapse imaging in a number of embryo model systems have revealed the complexity of neural crest migratory patterns (Blasky et al., 2014; Clay and Halloran, 2014; McGurk et al., 2014; Moosmann et al., 2014; Kulesa et al., 2013; Nishiyama et al., 2012). Neural crest cells may move collectively in sheets and chains, or as individuals in multicellular streams (McLennan and Kulesa, 2015). Regardless of the type of migration, neural crest cells follow stereotypical migratory pathways during prolonged movements to the periphery (persistence). Individual cell trajectories tend to be directed (linearity) within streams that maintain a discrete integrity (cohesion). Thus,

despite the wide variety of neural crest cellular phenomena, there are common features of neural crest cell migratory patterns that include persistence, linearity and cohesion.

To more rapidly test hypothetical mechanisms of neural crest cell persistence, linearity, and stream cohesion, computational models have been formulated from empirical data. These models include: (1) frontal expansion (Newgreen et al., 2013); (2) co-attraction/contact inhibition of locomotion (CIL) (Carmona-Fontaine et al., 2011) and; (3) cell-induced gradient (McLennan et al., 2012). The frontal expansion model is based on enteric neural crest cell dispersion and proliferation within open spaces of the developing gut (Young et al., 2004; Simpson et al., 2007). Time-lapse imaging of mouse enteric neural crest cells has revealed that advancing cells move with low directionality and are leap-frogged by trailer cells in a repeating pattern (Young et al., 2014). In contrast, the co-attraction and contact inhibition of locomotion (CIL) model proposes that secretion of a local chemoattractant by migrating neural crest cells prevents widespread dispersal and makes CIL more efficient to generate cell polarity and directed movement (Carmona-Fontaine et al., 2011; Woods et al., 2014). Lastly, we proposed a cell-induced gradient model in which lead neural crest cells respond to a chemotactic guidance signal and instruct trailer cells to follow (McLennan et al., 2012; McLennan, Schumacher et al., 2015). Together, these models that reflect the diverse characteristics of neural crest cell migratory patterns throughout the embryo are helping to shed light on underlying mechanisms.

The discoveries that chemotactic factors are present within the embryonic microenvironment changed the neural crest cell migration paradigm. These chemotactic factors include glial cell derived neurotrophic factor (GDNF) (Lake and Heuckeroth, 2013), platelet derived growth factor (PDGF) (Eberhart et al., 2008; He and Soriano, 2013), fibroblast growth factors (FGFs) (Sato et al., 2011) and vascular endothelial derived growth factor (VEGF) (McLennan et al., 2010), complement fragment c3a (Carmona-Fontaine et al., 2011), and stromal cell-derived factor 1 (SDF1) (Kasemeier-Kulesa et al., 2010; Saito et al., 2012; Theveneau et al., 2013). This evidence has led to questions about how neural crest cells interpret chemical signals both in their microenvironment and from/to each other to move in a directed manner and migrate as a coordinated population.

We previously showed that VEGF acts as a chemoattractant for neuropilin-1 expressing cranial neural crest cells in chick (McLennan et al., 2010). Loss of neuropilin-1 function caused neural crest cells to stop prior to entering the second branchial arch (McLennan and Kulesa, 2007). Computational modeling then predicted the presence of lead and trailer neural crest cells in the presence of a VEGF chemoattractant profile shaped by tissue growth and cell consumption, which we termed a cell-induced gradient model (McLennan et al., 2012). Gene profiling identified distinct expression patterns between lead and trailer neural crest cells (McLennan et al., 2012) that correlated with unique cell behaviors observed within each of these two subpopulations (Teddy and Kulesa, 2004). Tissue transplantations that placed trailer neural crest cells in advance of the leaders showed trailers adopted invasive behaviors and gene expression based on their

new stream position (McLennan et al., 2012). Further single- cell profiling has now identified a stable and consistent molecular signature unique to a subset of lead cells narrowly confined to the advancing migratory front, which we call trailblazers (McLennan, Schumacher et al., 2015). Whether VEGF is one of the microenvironmental signals that establishes lead and trailer neural crest cell identities, and how cells interpret the VEGF chemoattractant profile to move in a directed manner, remains unknown.

Here, we study these questions using the chick embryo model system and agent-based computational modeling. We first compare the gene expression profiles of migrating neural crest cells exiting from neural tube explant cultures to in vivo data. We examine the response of neural crest gene expression to timed addition and removal of VEGF in this assay. Based on these data, we implement an integrate-and-switch mechanism into our computational model and test cell migration efficiency as a function of switching times. To test the neural crest migratory response to alterations in the in vivo VEGF chemoattractant profile, we place ectopic sources of VEGF either adjacent or within the trailer portion of the stream and monitor alterations to cell trajectories, stream integrity, and gene expression. We test whether trailer neural crest cells require VEGF for guidance by morpholino knockdown of VEGF production in the ectoderm or by binding endogenous VEGF protein within the migratory pathway. Finally, we examine changes in lead neural crest cell gene expression in response to reduction in VEGF signaling either by binding up of endogenous VEGF or knockdown of the neuropilin1 receptor by siRNA.

Materials and Methods

Embryos, in ovo cell labeling and tissue transplantation

Fertilized white leghorn chicken eggs (supplied by Centurion Poultry Inc., Lexington, GA) were incubated at 38C in a humidified incubator until the desired HH (Hamburger and Hamilton, 1951) stage of development.

For VEGF transplant experiments, premigratory neural crest were labeled by injecting Vybrant DiO (V22889, Invitrogen, Carlsbad, CA) into the lumen of the neural tube. Embryos were then re-incubated for 12hrs to allow neural crest cells to exit the neural tube and form a discrete migratory stream. Clumps of DiI-labeled endothelial cells (control (CRL-2279, ATCC, Manassas, VA)) or VEGF-expressing cells (CRL-2460, ATCC) grown as hanging drop cultures were then transplanted either within or adjacent to the trailer subpopulation of the migrating neural crest stream. Manipulated embryos were either re-incubated for 1 hr and then mounted on glass bottom dishes (P35G-1.5-20-C, MatTek Corporation, Ashland, MA) for time-lapse imaging as previously described (Chapman et al., 2001; McKinney et al., 2013) or for 12 hrs before being harvested for static imaging and cell isolation for gene expression profiling as previously described (McLennan et al., 2012). For VEGF signaling knockdown experiments, neuropilin-1-Fc (566-NNS, R & D Systems, Inc.) targeted injections and neuropilin-1 siRNA electroporations were performed as previously described (Bron et al., 2004; McLennan and Kulesa, 2007). Control GFP (pMES) or fluorescently tagged VEGF morpholino (GeneTools, Philomath, OR) was targeted to the ectoderm directly overlying the trailer

neural crest cell subpopulation by injecting a small amount of construct or morpholino immediately above the cranial ectoderm on one side of the embryo at HH St 9-11, and then electroporated with platinum electrodes placed on either side of the embryo. After 24 hrs re-incubation, embryos were fixed, cryostat sectioned and HNK-1 immunohistochemistry was performed as previously described (McLennan et al., 2010).

In vitro assays

Cranial neural tubes (r2-r6) containing premigratory neural crest cells were cultured in vitro as previously described (McLennan et al., 2010). For the lead/trailer molecular analysis, neural tubes were plated on nuclease-free 1.0 PEN Membrane Slides (415190-9081-000, Zeiss, Jena, Germany) so that neural crest cells would migrate onto the slides and be easily and selectively isolated. After 24 hrs of incubation to allow for neural crest migration, slides were dehydrated with 100% ethanol for 5 minutes. Using a PALM Microbeam (Zeiss), neural crest cells adjacent to the neural tube (trailers) and at the edge of the invasive front (leaders) were catapulted without contact into an adhesive cap (415190-9181-000, Zeiss), lysed and used for RT-qPCR on an ABI 7900HT Fast Real-Time PCR system (ABI, Oyster Bay, NY). For the time-course exposure to VEGF, neural tubes were plated on glass bottom dishes, one neural tube per dish (3 dishes/replicates per condition/time point). After overnight incubation, with Ham's F-12 Nutrient Mix Media (11765054, Invitrogen, Grand Island, NY), neural tubes were removed leaving only neural crest cells. Ham's F-12 Nutrient Mix Media containing VEGF then replaced the plain media for 2 hours, and then the media was replaced with plain media (Fig. 3A). This media was then replaced with media

containing VEGF at different times (Fig. 3A). Neural crest cells were lysed directly on the glass bottom dishes at different time points by replacing media with 10ul of Cells-to-Ct lysis solution containing 1:100 DNAse I (4387299, Life Technologies-Invitrogen). The lysis reaction was halted, after 15 minutes at room temperature, with 1ul of Stop solution and samples were immediately placed on dry ice and stored at -80C.

Molecular profiling

cDNA was synthesized directly from sample lysates (438814, Life Technologies) in reactions that included 1ul of RNAse inhibitor (N261b, Promega, Madison, WI). Gene-specific targets were pre-amplified from a portion of the cDNA in 20ul preamp reactions using 14 thermal cycles according to a miniaturized version of Life Technologies' Cells-to-Ct preamp kit (4387299, Life Technologies). Pre-amplified products were diluted with 1X TE before being analyzed by microfluidic RT-qPCR on Fluidigm's Biomark HD platform. Non-logarithmic curves were manually removed in Biomark software. Data were normalized using three reference genes chosen from at least six candidates and analyzed with Biogazelle's qBASE software. To combat the variability inherent within our model system, we set statistical significance at $p<0.1$, choosing to include rather than exclude potential genes of interest. In lieu of multiple testing correction to eliminate potential false positives, we focused on genes that were implicated consistently in multiple analyses. Partek's Genomics Suite was employed for generating clusters, dissimilarity matrices and intensity plots.

Fluorescent in-situ hybridization chain reaction (HCR) mRNA expression analysis

Neural tubes were isolated and plated, 5-6 neural tubes per glass bottom dish and incubated overnight as described above. Cultures were fixed in 4% paraformaldehyde at room temperature for 1 hr and dehydrated stepwise with an ethanol/PBS-T gradient. Cultures were left overnight in ethanol and then rehydrated stepwise into PBS-T. FoxD3, Hand2 and Bambi mRNA transcripts were visualized simultaneously in neural crest cells in culture dishes placed on the confocal microscope stage and images collected using the same imaging settings for all cultures (LSM 710, Zeiss). HCR probes were used at a concentration of 2 nM and hairpins at a concentration of 30 nM.

Analysis of HCR fluorescence and neural crest cell behaviors

We calculated the intensity of HCR fluorescence in neural tube explant cultures as a measure of gene expression signal. For this analysis, regions of interest were identified either proximal or distal from each explanted neural tube (Fig. 1F). Within the regions of interest, we used the 'Surfaces' function of Imaris (Bitplane USA) to identify cells using the FoxD3 channel and then measured the mean intensity of all fluorescent channels within each surface. The box plots in Fig. 1F were generated by combining the mean intensities from all of the proximal or distal regions of interest. Plus signs indicate outliers, while the box plots and whiskers indicate the quartiles and range, respectively, of each data set.

Computational Modeling

To verify that our experimental observations are consistent with our hypotheses, we employ the hybrid computational model first described in McLennan et al. (2012), with agent-based representation of cells and a chemoattractant described by a continuous reaction-diffusion equation. Previously, we introduced modifications and improvements to the model (McLennan, Schumacher et al., 2015), which we further build upon in this work. For the integrate-and-switch mechanism, we introduced a variable that records how much signal each cell had sensed. This variable increases at a fixed rate when a chemoattractant gradient above the sensing accuracy threshold is sensed, and decreases otherwise, at rates inversely proportional to the parameters leader-to-trailer switching time, t_{LT}, and trailer-to-leader switching time, t_{TL}, respectively. Pseudocode and a table of parameters used can be found in the supplementary materials (Supplementary Model Information).

To represent transplants of ectopic VEGF, we altered the chemoattractant distribution in our model simulations. From t=12 hours (6 hours after the start of migration), the background chemoattractant production was increased in a subregion of the migratory domain. To represent placement of a VEGF source outside of the domain (adjacent to the stream), the chemoattractant production was increased in a thin strip of $1/20^{th}$ the width of the domain, and for placement within the stream, a region of half the domain-width was chosen. In both cases, the length of the transplant was $1/8^{th}$ of the domain length, and the absolute length increased with domain growth.

Results

Lead and trailer molecular profiles vary according to the embryonic microenvironment and do not exist in vitro

Using morphometric analysis and molecular profiling, we have previously shown that neural crest cells display different phenotypes and gene expression profiles that depend on position within a migratory stream: in particular, a stream is composed of at least two subpopulations, leaders and trailers (McLennan et al, 2012, 2015; Teddy and Kulesa, 2004). Here, we conducted experiments where, as far as possible, the influence of the microenvironment was removed to address whether these subpopulations are predetermined or regulated by the surrounding embryonic microenvironment. We excised neural tubes containing premigratory neural crest cells, allowed the neural crest cells to migrate out from the neural tubes in vitro and isolated cells from the invasive front (distal) and near the neural tube (proximal) to perform molecular profiling (Fig. 1A; Tables 1,2). Euclidean clustering showed that lead and trailer molecular profiles seen in vivo are drastically different to those seen in vitro (Fig. 1B). A Euclidean dissimilarity matrix intensity plot shows that in vitro trail and in vitro lead were the most similar to each other, while in vitro lead and in vivo lead were the least similar to one another (Fig. 1C).

When the molecular profiles were compared at the individual gene level, there were 11/58 genes that were upregulated in the lead for both in vitro and in vivo, but only one gene, RUNX2, that was upregulated in both (Fig. 1D). There were 9/58 genes upregulated in the trail in vivo and 5/58 genes upregulated in the trail in vitro but only

one gene, FOXD3, that was expressed at high levels in both (Fig. 1E). Thus, even though there were gene expression profile differences in vitro between cells at the invasive front compared to cells near the explanted neural tube, these profiles did not reflect the lead and trailer neural crest cell gene expression profiles we determined in vivo (McLennan et al., 2012).

To confirm our in vitro profiling results by expression analysis, we used fluorescent in-situ hybridization chain reaction (HCR) methodology to simultaneously observe HAND2, BAMBI, and FOXD3 in migrating neural crest cells (Fig. 1F). We found that FOXD3 was strongly expressed in migrating cells near the explanted neural tubes (Fig. 1G, red). In contrast, expression of HAND2 and BAMBI was very low throughout the entire migrating neural crest cells in vitro (Fig. 1G, green and yellow). Therefore, gene expression analyses by HCR agreed with our in vitro RT-qPCR profiling results and confirmed that the in vivo lead/trailer molecular signatures do not exist in vitro.

To investigate whether VEGF exposure in culture could influence the gene expression profile of migrating neural crest cells, we added VEGF to neural tube cultures overnight (Fig. 2A). Euclidean clustering and Euclidean dissimilarity matrix intensity plots showed that upon exposure to VEGF lead and trailer gene profiles in vitro were still very different to the lead and trail molecular signatures measured in vivo (Fig. 2B, C). Exposure to VEGF in lead neural crest cells in vitro induced significant expression of 14 genes examined (Fig. 2D). Of these 14, 9/14 were up- and 5/14 were down-regulated, compared to in vitro lead (distal) neural crest cells not exposed to VEGF (Fig. 2D).

Three of the genes that were upregulated are genes typically associated with the most invasive in vivo lead neural crest cells narrowly confined to the migratory front (termed ‘trailblazers’ in McLennan, Schumacher et al., 2015); NEDD9, BAMBI and NOTCH1 (Fig. 2D, purple). These experiments reveal that lead and trailer neural crest cell molecular signatures are an emergent property after exposure to signals within the embryonic neural crest microenvironment, one of which is VEGF.

Neural crest genes are rapidly induced in vitro in response to changes in VEGF

Tissue transplantations we previously performed in vivo (McLennan et al., 2012) showed that neural crest cells altered their gene expression profiles to correspond with new stream positions. We refined our computational model to reflect this, but it has remained unclear how rapidly neural crest cells could alter their expression profile and thus transition from a lead to trailer cell behavior or vice-versa. To determine the gene expression dynamics of neural crest cells to addition or removal of VEGF in culture, we performed a series of timed experiments. That is, neural tube cultures were exposed to VEGF for 2 hrs, then VEGF was removed for 90 min and re-applied for 90 min (Fig. 3A). Samples of neural crest cells for RNA isolation and profiling were taken at a set of non-linearly spaced time points, to cover the possible scales of a few minutes to over an hour (Fig. 3A; all timepoints indicated correspond to samples, Table 3). When the temporal expression of all genes was examined, we found that 17/25 (96 total genes analyzed) showed differential expression at $p<0.1$ and 9/25 showed a consistent change in expression within the first 4 minutes after removal and re-addition, respectively (Fig. 3B, C).

After the initial exposure to VEGF for two hours, 18 genes were significantly downregulated (Table 1). No genes in our set were significantly upregulated. When viewing the response time of genes to both removal and reapplication of VEGF, many genes responded to the removal of VEGF within four minutes, but then the response to reapplication of VEGF of those same genes varied greatly (Fig. 3C). Of the 18 genes, 14 genes had reoccurring responses upon removal and/or reapplication of VEGF. Six genes were significantly downregulated upon exposure to VEGF and then upregulated after removal of VEGF but displayed no significant change upon the reapplication of VEGF (Table 1, green). Two genes were significantly downregulated upon exposure to VEGF but with no significant change after removal of VEGF and significantly downregulated upon the reapplication of VEGF (Table 1, orange). Finally, six genes were significantly downregulated upon exposure to VEGF and then upregulated after removal of VEGF and then significantly downregulated upon the reapplication of VEGF (Fig. 3D, Table 1, purple). These data suggest that neural crest cell molecular profiles start to change in response to changes in VEGF within their surroundings in a matter of four minutes.

Computational model migration efficiency depends on behavior-switching timescales

To explore the sensitivity of our computational model to the rates of switching between leader and trailer behavior, as implemented in the integrate-and-switch mechanism (Fig. 4A), we calculated the average number of cells in the domain at t=24 hours, relative to

the non-switching case (McLennan, Schumacher et al., 2015), for different combinations of lead-to-follow and follow-to-lead switching times (Fig. 4B). Migration efficiency was higher when switching times were similar to each other (Fig. 4C). Outcome variability, measured as the coefficient of variation of cell number, was also lower for matched switching times (Fig. 4C). Migration was least efficient for slow follow-to-lead switching times (Fig. 4B). Together with the in vitro gene expression analysis, which shows fast response to VEGF removal in particular (Fig. 3C) and thus suggests fast lead-to-follow switching, this constrains our model to behavior-switching timescales on the order of a few minutes.

Trailer neural crest cells respond to ectopic VEGF

We have previously shown that lead neural crest cells can respond to and divert cell trajectories towards ectopic sources of VEGF placed adjacent to the migratory stream within typical cranial neural crest exclusion zones (McLennan et al., 2010). Our model simulations predict that trailer cells receive guidance instructions from leaders, rather than VEGF signals (McLennan et al., 2012). Thus, it has remained unclear whether trailer cells would respond or ignore an ectopic source of VEGF placed within or adjacent to the migratory stream. To address this, we waited until lead neural crest cells had migrated from the neural tube and placed ectopic sources of VEGF either adjacent to or within the trailer subpopulation of the stream (Fig. 5).

When an ectopic VEGF source was placed adjacent to the trailer subpopulation of the neural crest migratory stream, neural crest cells rerouted towards the VEGF source

(Fig. 5B compared to Fig. 5A). Neither lead nor trailer neural crest cells were attracted to control cells transplanted into the same region (data not shown; McLennan et al, 2010). Static images suggested that neural crest cells originating from r3 and r4 diverted cell trajectories to move towards the ectopic VEGF source (Fig. 5B). Time-lapse imaging confirmed this and revealed r4 trailer neural crest cells in close proximity to the ectopic VEGF source diverted trajectories (Fig. 6A, 6B, 6E).

In both time-lapse imaging and static analyses we saw a small number of trailer neural crest cells leave the migratory stream in response to VEGF (Fig. 5G). Neural crest cells that remained in the migratory route clustered near the ectopic VEGF-source (Fig. 6B). The width of the stream was significantly increased when ectopic VEGF was placed adjacent to the trailer portion of the stream (Fig. 5H). Neural crest cells still migrated the entire length of the migratory route; hence the migration of the lead neural crest cell subpopulation was unaffected (Fig. 5B). High resolution time-lapses of neural crest cells prelabeled with a membrane marker showed that trailer neural crest cells remained reasonably immobile within the proximal portion of the stream while sending multiple filopodial protrusions towards the ectopic VEGF (data not shown).

To determine whether trailer neural crest cells would respond to changes in VEGF signals after receiving hypothetical instructions from leaders, we placed an ectopic VEGF source within the trailer subpopulation of cells (Fig. 6C, 5C compared to 5A). We found that the trailer neural crest cells clustered around the ectopic VEGF source on both the proximal and distal sides of the source (Fig. 5C, 6D, 6F). We also found the

inclusion of an ectopic VEGF source within the trailer subpopulation increased the width of the neural crest migratory stream near the transplant site (Fig. 5H). This was not due to cells treating the tissue transplant as a barrier, since some migrating neural crest cells could be observed to be within the transplant (Fig. 5D, Fig. 6D,F). Furthermore, lead neural crest cells were still able to migrate normally the entire length of the migratory route (Fig. 5C). These results reveal that trailer neural crest cells can respond to VEGF, but prefer to remain within their zone of the migratory stream if possible.

Altering the chemoattractant distribution in model simulations causes break-up of the migratory stream

To test whether the observed effects of transplanting ectopic VEGF could be explained by our model with the integrate-and-switch mechanism, we computationally represented the tissue transplantation experiments (Fig. 5D-F). In the region of increased chemoattractant production, model simulations showed that trailer cells increasingly switched to become leader cells compared to the control simulations (Fig. 5E,F; Movies, 1,2). This clustering of cells around the transplants resulted in a break-up of the stream into a distal-moving subpopulation that interacted with the ectopic chemoattractant (Fig. 5E,F,I; Movies 1, 2). Thus, the effects of perturbing the VEGF distribution in vivo are consistent with our cell-induced gradient model with VEGF-induced cell behavior switching.

Trailer neural crest cells near ectopic sources of VEGF upregulate genes associated with trailblazers

To determine whether the trailer neural crest cells that responded to ectopic sources of VEGF changed their gene expression, we examined cells in physical contact with the ectopic sources of VEGF (Fig. 7A). Euclidean clustering revealed that neural crest cells in contact with an ectopic source of VEGF placed within the trailer subregion of the migratory stream were most similar to wildtype trailer neural crest cells (Fig. 7B,C). We found there was a significant upregulation in the expression of nine genes in response to the presence of VEGF (Fig. 7D). This included the expression of four genes (CCR9, CXCR1, PKP2, and BAMBI) (Fig. 7D), which we previously determined to be upregulated in trailblazers (McLennan, Schumacher et al., 2015). Together, this suggested that neural crest cells that encountered an ectopic VEGF source placed within the trailer subpopulation upregulated a subset of lead cell genes but, for the most part, retained similarity to trailer cells.

When neural crest cells diverted away from the typical migratory pathway to encounter an ectopic VEGF source placed adjacent to the stream, we found their gene expression profile changes (Fig. 7B,C). There were 22 genes that were significantly upregulated in the neural crest cells responding to VEGF (Fig. 7E). This list includes eight genes (CCR9, CXCR1, PKP2, BAMBI, CXCR7, NOTCH1, EPHB1 and CTNNB1) that are in the molecular signature of the trailblazers (Fig. 7E, purple). Thus, neural crest cells that diverted away from the discrete stream to interact with an ectopic VEGF source had a

higher number of lead genes induced and four of these genes were shared with cells that encounter VEGF within the stream.

Trailer neural crest migration is unaffected by a reduction in VEGF signaling

Our hypothesis states that trailer neural crest cells do not require VEGF signaling for guidance, but instead receive guidance instructions from lead cells. To test this, we knocked down VEGF function in the ectoderm directly overlying only the trailer portion of the neural crest migratory stream using targeted VEGF morpholino (Fig. 8A). Knocking down VEGF in the surface ectoderm had no effect on the width of the trailer neural crest cell subpopulation when we compared the stream width to control embryos (Fig. 8A). In addition, when we bound up soluble VEGF protein in the trailer mesoderm by injecting Np1-Fc into the tissue, we found no effect to the trailer neural crest subpopulation (Fig. 8B). These results indicated that VEGF is not required for proper migration of the trailer cell population.

Lead molecular profiles are altered after reduction in VEGF signaling

We have previously shown that Np1 siRNA transfected neural crest cells exhibited reduced migration to the branchial arch target site (McLennan and Kulesa, 2007). To determine whether a reduction in cellular VEGF signaling significantly influenced the molecular profile of lead neural crest cells, we electroporated neural crest cells with Np1 siRNA and isolated these cells for RT-qPCR. We compared the molecular profiles of lead and trailer neural crest cells transfected with Np1 siRNA to lead, middle and trailer neural crest cells transfected with control EGFP. We determined that lead Np1 siRNA

neural crest cells were most similar in gene expression profile to neural crest cells positioned mid-stream (Fig. 9A,C). Trailer Np1 siRNA neural crest cells were most similar to trailer control neural crest cells (Fig. 9A,C).

When we knocked down available VEGF by binding up endogenous VEGF with Np1-Fc injections into and around the migratory stream, we found that lead Np1-Fc neural crest cells were most similar to lead control neural crest cells (Fig. 9B,D). Trailer Np1-Fc neural crest cells were most similar to trailer control neural crest cells (Fig. 9B,D).

Comparison of specific genes that were up- or down-regulated in lead neural crest cells after VEGF signaling reduction revealed that lead Np-1 siRNA neural crest cells down-regulated only two genes; one of these was associated with the invasive trailblazers (Fig. 9E). There were 11 up-regulated genes, four of which we have associated with the trailblazers (Fig. 9E). In comparison, Np1-Fc injections resulted in only one up-regulated gene and eight down-regulated genes in lead cells, four of which are associated with the trailblazer signature (Fig. 9E). Together, these data show that knockdown of VEGF signaling by two distinct methods altered the expression profile in lead neural crest cells in distinct ways suggesting that there are different cell responses to loss of VEGF signaling.

Discussion

We used the chick embryo system and computational modeling to study the importance of VEGF during neural crest cell migration in the head. We demonstrated that distinct gene expression profiles of lead and trailer neural crest cells do not exist in vitro. However, exposure to VEGF in culture caused an upregulation of a small subset of trailblazer genes. Further, timed addition and removal of VEGF in culture showed neural crest gene expression profiles change within minutes and provided the basis for incorporation of an integrate-and-switch mechanism into our computational model. Model simulations predict that migration efficiency is influenced by lead-to-trailer behavior-switching timescales. We also showed that presentation of ectopic VEGF sources to trailer cells altered cell trajectories and gene expression, consistent with in silico predictions, but loss of VEGF signals in the trailer region did not. We conclude that VEGF and other microenvironmental signals are critical to establish lead neural crest cells that read out guidance signals and instruct trailers to follow.

Signals within the in vivo microenvironment, rather than from the neural tube, establish distinct lead and trailer neural crest cell molecular signatures in the head. By analyzing gene expression in cranial neural crest cells that emigrated from neural tube explant cultures (Fig. 1), we found no evidence of either a trailblazer (McLennan, Schumacher et al., 2015) or lead cell signature (McLennan et al., 2012). Rather, neural crest cell gene expression profiles were independent of the distance migrated in the culture dish (Fig. 1). mRNA expression analysis followed by quantitation of fluorescence signals in individual migrating neural crest cells confirmed the lack of expression of key genes

previously correlated with in vivo leaders (Fig. 1F,G). The only exception to this was Runx2 (upregulated in leaders) and FoxD3 (upregulated in trailers), suggesting that the expression of these two genes may be endowed by signals within the neural tube (Fig. 1B-D).

Exposure of VEGF to neural tube explant cultures partially recovered the expression of genes associated with in vivo lead neural crest cells, including three trailblazer genes (Fig. 2; Bambi, Notch1, and Nedd9; McLennan, Schumacher et al., 2015). This suggested that VEGF may be one of the in vivo microenvironmental signals that establish a distinct trailblazer neural crest cell molecular signature. Of these trailblazer genes, elevated expression of Nedd9 has been associated with metastatic activity in several aggressive cancers (Li et al., 2014; Zhang et al., 2014; Wang et al., 2014). Nedd9 has been shown to be critical to cancer cell invasion due to its ability to stimulate cells to undergo an epithelial-to-mesenchymal transition, attachment to the extracellular matrix and migratory speed, when analyzed in vitro (Zhong et al., 2014; Jin et al., 2014; Sima et al., 2013). Further studies of VEGF and the trailblazer genes, including Nedd9, may reveal the interplay between VEGF stimulation and the functional role of these genes in neural crest migration.

Our computational model included a phenotypic switch from lead to trailer cell phenotype, the simulations of which predicted cell migration efficiency is influenced by switching timescales. By analyzing gene expression dynamics after timed addition and removal of VEGF in vitro, we observed a rapid and significant change in neural crest

cell gene expression within four minutes (Figs. 3,4). From these data, we parametrized our newly extended model so that lead cells become trailers after they fail to read out an appropriate level of VEGF over a short number of time steps. Simulations of our previous model (McLennan et al., 2012) compared to the new integrate-and-switch mechanism identified two model features that made migration more robust to intrinsic variability, such as: (1) a non-zero timescale of switching between leader and trailer cell states; and (2) hysteresis, or a memory, which decays with time, of the signal sensed (the directional cue). Thus, the integrate-and-switch mechanism, as presented here, provided the simplest extension to our existing model that captured the plasticity of neural crest cell behavioral identity and did so robustly. It is important to note that the integrate-and-switch mechanism in fact makes our model of neural crest cell migration less complex, in the sense that the size of the lead subpopulation does not need to be pre-specified, but emerges from the interactions of the cells with the chemoattractant distribution.

Trailer neural crest cells altered trajectories and gene expression in response to an ectopic source of VEGF, suggesting the trailer phenotype and gene expression profile is not hard-wired. When ectopic VEGF was placed adjacent to the trailer subpopulation (in the region adjacent to r3), some trailer neural crest cells diverted away from the stream towards the ectopic VEGF source (Fig. 6). Diverted trailer cells that encountered the ectopic VEGF source had significant changes in gene expression, including upregulation of 22 genes, 8 of which were trailblazer signature genes (Fig. 7).

Similarly, ectopic VEGF placed within the trailer subpopulation caused newly exiting cells to stop and interact with the VEGF source and distal cells to reverse direction to move back to the VEGF source (Fig. 6). Neural crest cells that encountered ectopic VEGF upregulated nine genes typically associated with the invasive front (Fig. 7). Four trailblazer signature genes were commonly upregulated (Bambi, Ccr9, Cxcr1, Pkp2) in the ectopic VEGF source transplantations. The chemokine receptors Ccr9 and Cxcr1 have been implicated in aggressive cancers (Johnson-Holiday et al., 2011; Heinrich et al., 2013; Amersi et al., 2008), suggesting correlation with an invasive cell type. VEGF directly stimulated the expression of Cxcr1 and Ccr9 in trailer cells in response to ectopic VEGF (Fig. 7), but not in the presence of VEGF in vitro (Fig. 2). Whether the upregulation of Cxcr1 in trailer neural crest cells in response to ectopic VEGF also suggests the presence of the ligand IL8 is unknown. The Cxcr1/Il8 axis has been implicated in a number of invasive cell migration events including mesenchymal stem cell migration to gliomas (Chen et al., 2014) and in neutrophil chemotaxis (Oehlers et al., 2010).

Model simulations predicted that neural crest cells that diverted towards ectopic VEGF sources switched from trailer to leader, resulting in alterations to stream morphology that agreed with experimental results (Fig. 5; Movies 1,2). When VEGF was knocked down in either the ectoderm overlaying the trailer portion of the stream (reduce VEGF production) or the mesoderm (bind up existing VEGF protein), there was no effect on trailer neural crest cell migration (Fig. 8). This suggested that VEGF signals are not

required for guidance of trailer neural crest cells, which instead may rely on cell contact or unknown microenvironmental signals for guidance.

In summary, our findings identify the importance of VEGF as one of the in vivo microenvironmental signals that establish a distinct subpopulation of lead neural crest cells. VEGF signals do not provide guidance cues to trailer neural crest cells, but convert trailers to lead cells that alter cell trajectories and gene expression when a VEGF source is introduced ectopically. These data support our cell-induced gradient model in which microenvironmental signals define and direct lead neural crest cells that instruct trailers to follow. Inclusion of an integrate-and-switch mechanism in silico, through which lead neural crest cells become trailers and vice-versa, has a distinct timescale of switching to promote model migration efficiency. Together, these steps appear essential to promote neural crest cell persistence and stream cohesion. Further analysis of the cell behaviors and gene expression changes in neural crest cells that respond to ectopic VEGF sources may help to identify other microenvironmental guidance signals and the mechanistic underpinnings by which lead cells instruct trailers to follow.

Acknowledgements: PMK would like to acknowledge kind and generous funding from the Stowers Institute for Medical Research. We also thank members of the BioInformatics, Histology and Molecular Biology core facilities at the Stowers Institute for Medical Research. Fluidigm Biomark HD dynamic arrays were analyzed at the Children's Hospital Boston IDDRC Molecular Genetics facility. LJS would like to acknowledge the UK Engineering and Physical Sciences Research Council for funding through a studentship at the Life Science Interface programme of the University of Oxford's Doctoral Training Centre and thank Michael Bentley, Fred Hoffmann, Victoria Hore, Allon Klein and Ben MacArthur for discussions.

Figure Legends

Figure 1: Neural crest cells do not maintain lead and trailing molecular profiles in vitro. (A) Schematic of in vitro and in vivo neural crest isolation from proximal and distal regions. (B-C) Euclidean clustering and dissimilarity matrix plot of proximal and distal molecular profiles isolated from in vitro and in vivo samples. (D) Venn diagram of genes significantly upregulated in distal neural crest cells. (E) Venn diagram of genes significantly upregulated in proximal neural crest cells. (F) HCR of neural crest cells grown in vitro, probed for FOXD3, HAND2 and BAMBI. (G) Mean fluorescence intensity of the HCR probes. nt, neural tube, r4, rhomobomere 4, 24h, 24 hours, LCM, laser capture microdissection, RTqPCR, reverse transcription quantitative polymerase chain reaction, FL, fluorescence.

Figure 2: Neural crest cells upregulate genes typically associated with the migratory invasive front when exposed to VEGF. (A) Schematic of experimental design. (B, C) Euclidean clustering and Euclidean dissimilarity matrix plot of distal and proximal molecular profiles isolated from in vitro samples after addition of VEGF and compared to in vivo samples. (D) Genes significantly upregulated and downregulated in distal in vitro neural crest cells upon exposure to VEGF compared to lead neural crest cells in vivo. Purple highlight indicates genes associated with the neural crest cell trailblazers. nt, neural tube, r4, rhombomere 4, 24h, 24 hours, LCM, laser capture microdissection, RTqPCR, reverse transcription quantitative polymerase chain reaction.

Figure 3: Response of neural crest cell molecular profiles to VEGF. (A) Experimental time-course. (B) Individual and average response (weighted by the inverse error in the mean) of genes with significant ($p<0.1$) and consistent (repeated across three experimental conditions) differential expression. Error bars show weighted sample deviation. (C) Summary of first response times of genes after removal and readdition of VEGF. (D) Relative changes in expression of genes responding within four minutes under both conditions. r4, rhombomere 4, nt, neural tube

Figure 4: Model migration efficiency is influenced by behavior-switching timescales. (A) Schematic of integrate-and-switch model for leader-trailer transitions. (B) Effect of switching times on model migration efficiency (defined as the average number of cells after t=24 hours (n=20 simulations), relative to the maximum for the non-switching case (as in McLennan, Schumacher et al., 2015). Point spacing indicates parameter combinations sampled. White contours show >20% coefficient of variation, grey contours >30%. (C) Migration efficiency (solid lines) and coefficient of variation (dashed lines) as a function of the ratio of switching times.

Figure 5: Trailing neural crest cells respond to VEGF in vivo. (A) Cranial neural crest stream labeled with DiO (green) (n=18 embryos). (B) VEGF-expressing cells (red) were transplanted adjacent to trailing portion of the cranial neural crest stream (green) (n=12 embryos). (C) Ectopic VEGF cell transplant (red) placed within the trailing portion of the cranial neural crest stream (green) (n=11 embryos). (D) Representative control model simulation. (E) Representative model simulation with increased chemoattractant production at bottom left edge of domain from t=12 hours onwards. (F) Representative model simulation with increased chemoattractant production at bottom left area from t=12 hours onwards. (G) Average number of neural crest cells found in area adjacent to r3. (H) Width of the stream at the transplant. (I) Migration profiles of control and perturbed simulations, averaged over n=20 simulations.

Figure 6: Trailing neural crest cells reroute towards VEGF in vivo. (A, C) Schematic representations showing placement of the VEGF-expressing cells. (B) Selected images from a typical time-lapse imaging session showing neural crest cells responding to VEGF-expressing cells (red) transplanted adjacent to the trailing stream (green).(D) Selected images from a typical time-lapse imaging session showing neural crest cells responding to VEGF-expressing cells (red) transplanted within the trailing stream (green). (E) Examples of neural crest cell tracks in response to VEGF from timelapse shown in B. (F) Examples of neural crest cell tracks in response to VEGF from timelapse shown in (D). r4, rhombomere 4.

Figure 7: Trailing neural crest upregulate trailblazer genes in response to VEGF. (A) Schematic representation of the experiment. (B-C) Euclidean clustering and Euclidean dissimilarity matrix intensity plot of neural crest cells responding to VEGF. (D, E) Genes significantly upregulated in response to VEGF placed within (D) and adjacent (E). Purple highlight indicates genes typically associated with the neural crest cell trailblazers.

Figure 8: Trailing neural crest cell migration is not dependent on VEGF. (A) Schematic representation of experimental design of transfecting ectoderm with VEGF morpholino, transverse section of the trailing neural crest migratory stream (green) with VEGF morpholino electroporated into the overlaying ectoderm (red), width of the trailing portion of the migratory stream after ectoderm transfections. (B) Schematic representation of experimental design of injecting Np1-Fc into the trailing mesenchyme, transverse section of the trailing neural crest migratory stream (green) after Np1-Fc injection, width of the trailing portion of the migratory stream after Np1-Fc injections. r4, rhombomere 4, MO, morpholino.

Figure 9: Lead neural crest cells change their molecular profiles in response to perturbed VEGF signaling. (A, C) Euclidean clustering and Euclidean dissimilarity matrix plot of neural crest cells transfected with Np1 siRNA. (B, D) Euclidean clustering and Euclidean dissimilarity matrix plot of neural crest cells after Np1-Fc injections. (E) Genes significantly altered after VEGF signaling perturbations. Purple highlight indicates genes typically associated with the neural crest cell trailblazers.

Movie legends

Movie 1: Computer model simulation of the transplantation of an ectopic VEGF source placed adjacent to the cranial neural crest cell migratory stream. The movie sequence starts at the moment of transplant from a reference simulation (such that it is identical to

the control up to the moment of transplantation). In the simulations, VEGF is transplanted with the tissue such that the concentration is high and the area is highlighted.

Movie 2: Computer model simulation of the transplantation of an ectopic VEGF source placed within the trailer subpopulation cranial neural crest cell migratory stream.

References

Amersi, F. F., Terando, A. M., Goto, Y., Scolyer, R. A., Thompson, J. F., Tran, A. N., Faries, M. B., Morton, D. L., Hoon, D. S., 2008. Activation of CCR9/CCL25 in cutaneous melanoma mediates preferential metastasis to the small intestine. Clin Cancer Res. 14**,** 638-45.

Blasky, A. J., Pan, L., Moens, C. B., Appel, B., 2014. Pard3 regulates contact between neural crest cells and the timing of Schwann cell differentiation but is not essential for neural crest migration or myelination. Dev Dyn. 243**,** 1511-23.

Bron, R., Eickholt, B. J., Vermeren, M., Fragale, N., Cohen, J., 2004. Functional knockdown of neuropilin-1 in the developing chick nervous system by siRNA hairpins phenocopies genetic ablation in the mouse. Dev Dyn. 230**,** 299-308.

Butler Tjaden, N. E., Trainor, P. A., 2013. The developmental etiology and pathogenesis of Hirschsprung disease. Transl Res. 162**,** 1-15.

Carmona-Fontaine, C., Theveneau, E., Tzekou, A., Tada, M., Woods, M., Page, K. M., Parsons, M., Lambris, J. D., Mayor, R., 2011. Complement fragment C3a controls mutual cell attraction during collective cell migration. Dev Cell. 21**,** 1026-37.

Chapman, S. C., Collignon, J., Schoenwolf, G. C., Lumsden, A., 2001. Improved method for chick whole-embryo culture using a filter paper carrier. Dev Dyn. 220**,** 284-9.

Chen, L., Fan, J., Chen, H., Meng, Z., Chen, Z., Wang, P., Liu, L., 2014. The IL-8/CXCR1 axis is associated with cancer stem cell-like properties and correlates with clinical prognosis in human pancreatic cancer cases. Sci Rep. 4**,** 5911.

Clay, M. R., Halloran, M. C., 2014. Cadherin 6 promotes neural crest cell detachment via F-actin regulation and influences active Rho distribution during epithelial-to-mesenchymal transition. Development. 141**,** 2506-15.

Cordero, D. R., Brugmann, S., Chu, Y., Bajpai, R., Jame, M., Helms, J. A., 2011. Cranial neural crest cells on the move: their roles in craniofacial development. Am J Med Genet A. 155A**,** 270-9.

Eberhart, J. K., He, X., Swartz, M. E., Yan, Y. L., Song, H., Boling, T. C., Kunerth, A. K., Walker, M. B., Kimmel, C. B., Postlethwait, J. H., 2008. MicroRNA Mirn140 modulates Pdgf signaling during palatogenesis. Nat Genet. 40**,** 290-8.

Hamburger, V., Hamilton, H. L., 1951. A series of normal stages in the development of the chick embryo. J Morphol. 88**,** 49-92.

He, F., Soriano, P., 2013. A critical role for PDGFRalpha signaling in medial nasal process development. PLoS Genet. 9**,** e1003851.

Heinrich, E. L., Arrington, A. K., Ko, M. E., Luu, C., Lee, W., Lu, J., Kim, J., 2013. Paracrine Activation of Chemokine Receptor CCR9 Enhances The Invasiveness of Pancreatic Cancer Cells. Cancer Microenviron. 6**,** 241-5.

Jin, Y., Li, F., Zheng, C., Wang, Y., Fang, Z., Guo, C., Wang, X., Liu, H., Deng, L., Li, C., Wang, H., Chen, H., Feng, Y., Ji, H., 2014. NEDD9 promotes lung cancer metastasis through epithelial-mesenchymal transition. Int J Cancer. 134**,** 2294-304.

Johnson-Holiday, C., Singh, R., Johnson, E., Singh, S., Stockard, C. R., Grizzle, W. E., Lillard, J. W., Jr., 2011. CCL25 mediates migration, invasion and matrix

metalloproteinase expression by breast cancer cells in a CCR9-dependent fashion. Int J Oncol. 38**,** 1279-85.
Kasemeier-Kulesa, J. C., McLennan, R., Romine, M. H., Kulesa, P. M., Lefcort, F., 2010. CXCR4 controls ventral migration of sympathetic precursor cells. J Neurosci. 30**,** 13078-88.
Kulesa, P. M., McKinney, M. C., McLennan, R., 2013. Developmental imaging: the avian embryo hatches to the challenge. Birth Defects Res C Embryo Today. 99**,** 121-33.
Lake, J. I., Heuckeroth, R. O., 2013. Enteric nervous system development: migration, differentiation, and disease. Am J Physiol Gastrointest Liver Physiol. 305**,** G1-24.
Li, P., Zhou, H., Zhu, X., Ma, G., Liu, C., Lin, B., Mao, W., 2014. High expression of NEDD9 predicts adverse outcomes of colorectal cancer patients. Int J Clin Exp Pathol. 7**,** 2565-70.
Maguire, L. H., Thomas, A. R., Goldstein, A. M., 2015. Tumors of the neural crest: Common themes in development and cancer. Dev Dyn. 244**,** 311-22.
McGurk, P. D., Lovely, C. B., Eberhart, J. K., 2014. Analyzing craniofacial morphogenesis in zebrafish using 4D confocal microscopy. J Vis Exp. e51190.
McKeown, S. J., Wallace, A. S., Anderson, R. B., 2013. Expression and function of cell adhesion molecules during neural crest migration. Dev Biol. 373**,** 244-57.
McKinney, M. C., Fukatsu, K., Morrison, J., McLennan, R., Bronner, M. E., Kulesa, P. M., 2013. Evidence for dynamic rearrangements but lack of fate or position restrictions in premigratory avian trunk neural crest. Development. 140**,** 820-30.
McLennan, R., Dyson, L., Prather, K. W., Morrison, J. A., Baker, R. E., Maini, P. K., Kulesa, P. M., 2012. Multiscale mechanisms of cell migration during development: theory and experiment. Development. 139**,** 2935-44.
McLennan, R., Kulesa, P. M., 2007. In vivo analysis reveals a critical role for neuropilin-1 in cranial neural crest cell migration in chick. Dev Biol. 301**,** 227-39.
McLennan, R., Schumacher, L. J., Morrison, J. A., Teddy, J. M., Ridenour, D. A., Box, A. C., Semerad, C. L., Li, H., McDowell, W., Kay, D., Maini, P. K., Baker, R. E., Kulesa, P. M., 2015. Neural crest migration is driven by a few trailblazer cells with a unique molecular signature narrowly confined to the invasive front. Development. 142**,** 2014-25.
McLennan, R., Teddy, J. M., Kasemeier-Kulesa, J. C., Romine, M. H., Kulesa, P. M., 2010. Vascular endothelial growth factor (VEGF) regulates cranial neural crest migration in vivo. Dev Biol. 339**,** 114-25.
Moosmann, J., Ershov, A., Weinhardt, V., Baumbach, T., Prasad, M. S., LaBonne, C., Xiao, X., Kashef, J., Hofmann, R., 2014. Time-lapse X-ray phase-contrast microtomography for in vivo imaging and analysis of morphogenesis. Nat Protoc. 9**,** 294-304.
Newgreen, D. F., Dufour, S., Howard, M. J., Landman, K. A., 2013. Simple rules for a "simple" nervous system? Molecular and biomathematical approaches to enteric nervous system formation and malformation. Dev Biol. 382**,** 305-19.
Nishiyama, C., Uesaka, T., Manabe, T., Yonekura, Y., Nagasawa, T., Newgreen, D. F., Young, H. M., Enomoto, H., 2012. Trans-mesenteric neural crest cells are the principal source of the colonic enteric nervous system. Nat Neurosci. 15**,** 1211-8.

Oehlers, S. H., Flores, M. V., Hall, C. J., O'Toole, R., Swift, S., Crosier, K. E., Crosier, P. S., 2010. Expression of zebrafish cxcl8 (interleukin-8) and its receptors during development and in response to immune stimulation. Dev Comp Immunol. 34**,** 352-9.

Saito, D., Takase, Y., Murai, H., Takahashi, Y., 2012. The dorsal aorta initiates a molecular cascade that instructs sympatho-adrenal specification. Science. 336**,** 1578-81.

Sato, A., Scholl, A. M., Kuhn, E. N., Stadt, H. A., Decker, J. R., Pegram, K., Hutson, M. R., Kirby, M. L., 2011. FGF8 signaling is chemotactic for cardiac neural crest cells. Dev Biol. 354**,** 18-30.

Sima, N., Cheng, X., Ye, F., Ma, D., Xie, X., Lu, W., 2013. The overexpression of scaffolding protein NEDD9 promotes migration and invasion in cervical cancer via tyrosine phosphorylated FAK and SRC. PLoS One. 8**,** e74594.

Simpson, M. J., Zhang, D. C., Mariani, M., Landman, K. A., Newgreen, D. F., 2007. Cell proliferation drives neural crest cell invasion of the intestine. Dev Biol. 302**,** 553-68.

Teddy, J. M., Kulesa, P. M., 2004. In vivo evidence for short- and long-range cell communication in cranial neural crest cells. Development. 131**,** 6141-51.

Theveneau, E., Mayor, R., 2012. Neural crest delamination and migration: from epithelium-to-mesenchyme transition to collective cell migration. Dev Biol. 366**,** 34-54.

Theveneau, E., Steventon, B., Scarpa, E., Garcia, S., Trepat, X., Streit, A., Mayor, R., 2013. Chase-and-run between adjacent cell populations promotes directional collective migration. Nat Cell Biol. 15**,** 763-72.

Wang, H., Mu, X., Zhou, S., Zhang, J., Dai, J., Tang, L., Xiao, L., Duan, Z., Jia, L., Chen, S., 2014. NEDD9 overexpression is associated with the progression of and an unfavorable prognosis in epithelial ovarian cancer. Hum Pathol. 45**,** 401-8.

Woods, M. L., Carmona-Fontaine, C., Barnes, C. P., Couzin, I. D., Mayor, R., Page, K. M., 2014. Directional collective cell migration emerges as a property of cell interactions. PLoS One. 9**,** e104969.

Young, H. M., Bergner, A. J., Anderson, R. B., Enomoto, H., Milbrandt, J., Newgreen, D. F., Whitington, P. M., 2004. Dynamics of neural crest-derived cell migration in the embryonic mouse gut. Dev Biol. 270**,** 455-73.

Young, H. M., Bergner, A. J., Simpson, M. J., McKeown, S. J., Hao, M. M., Anderson, C. R., Enomoto, H., 2014. Colonizing while migrating: how do individual enteric neural crest cells behave? BMC Biol. 12**,** 23.

Zhang, Q., Wang, H., Ma, Y., Zhang, J., He, X., Ma, J., Zhao, Z. S., 2014. Overexpression of Nedd9 is a prognostic marker of human gastric cancer. Med Oncol. 31**,** 33.

Zhong, J., Bach, C. T., Shum, M. S., O'Neill, G. M., 2014. NEDD9 regulates 3D migratory activity independent of the Rac1 morphology switch in glioma and neuroblastoma. Mol Cancer Res. 12**,** 264-73.

Figure 1

Click here to download high resolution image

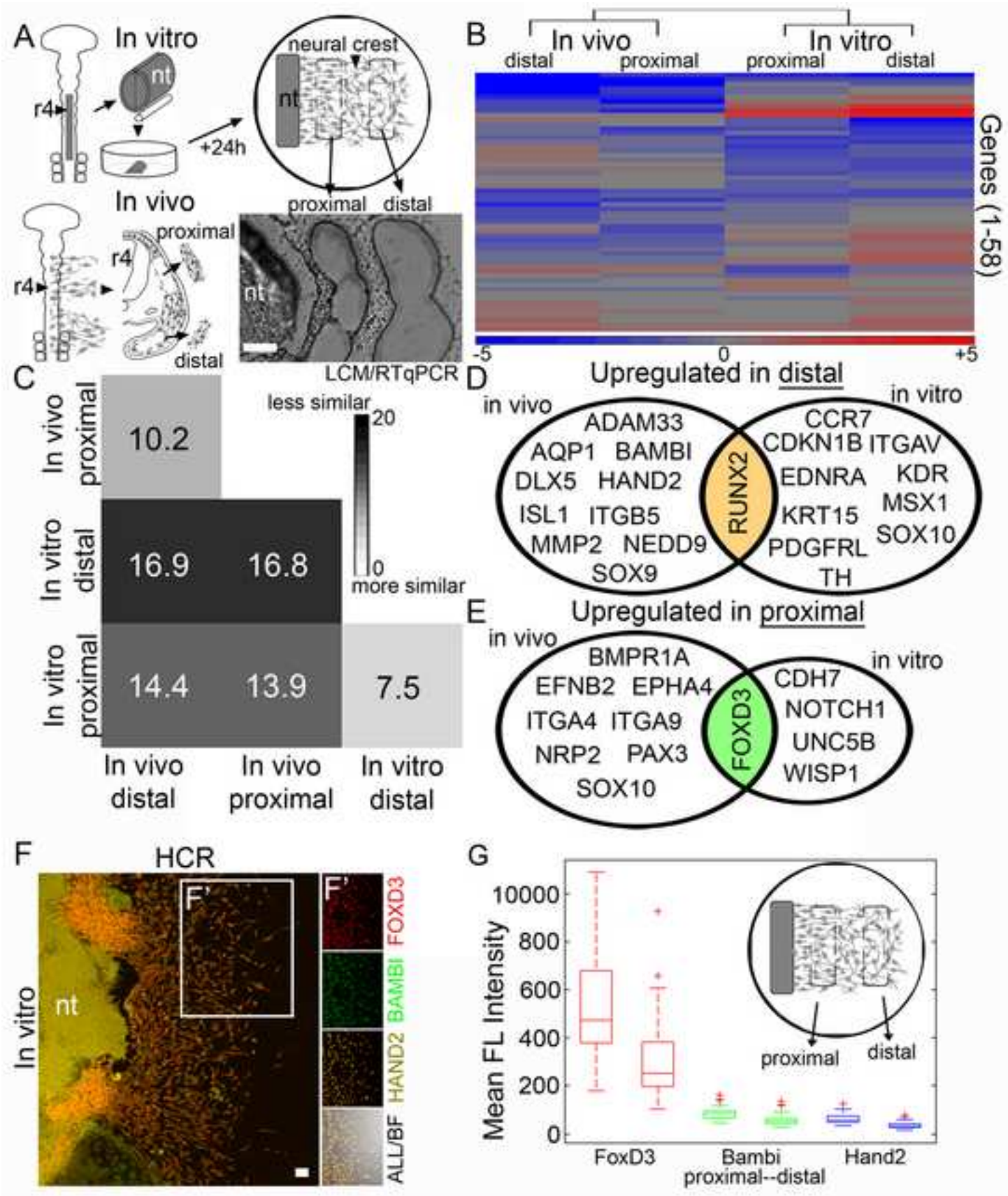

Figure 2

Click here to download high resolution image

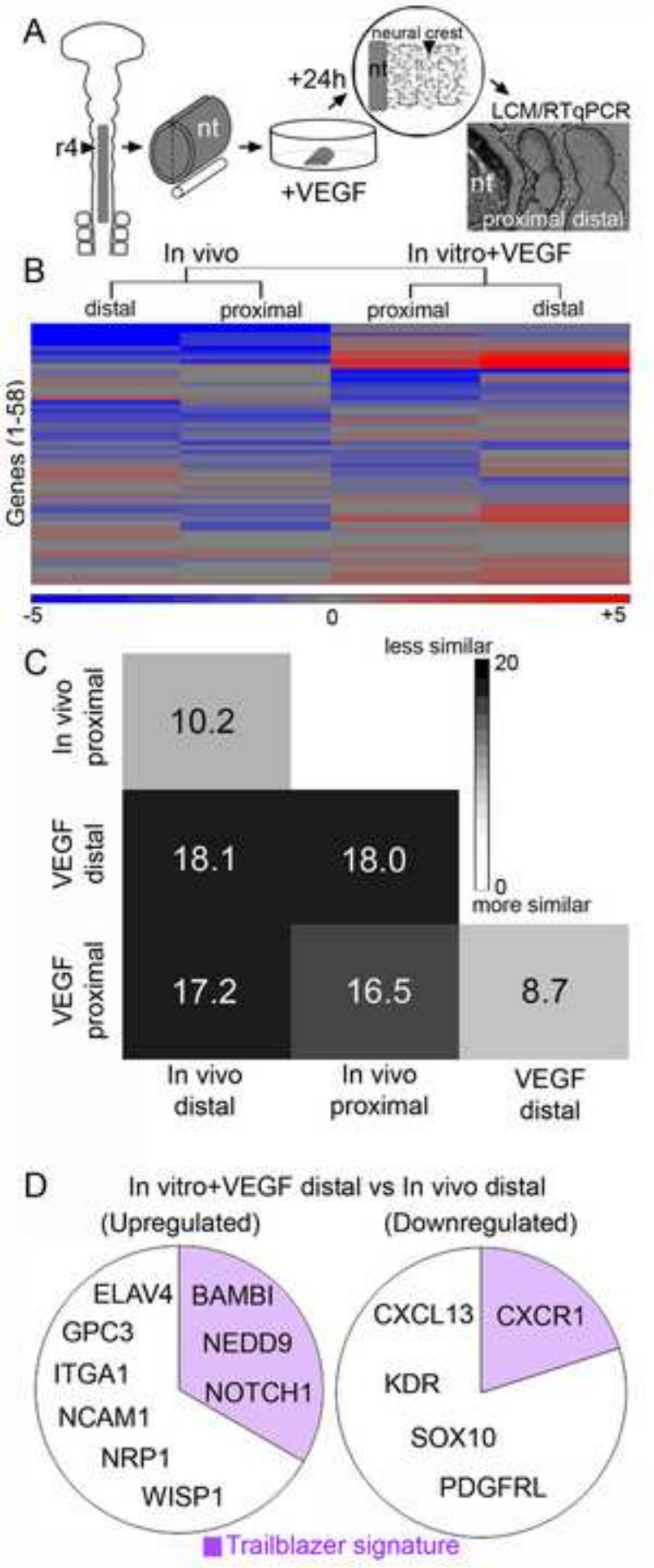

Figure 3

Click here to download high resolution image

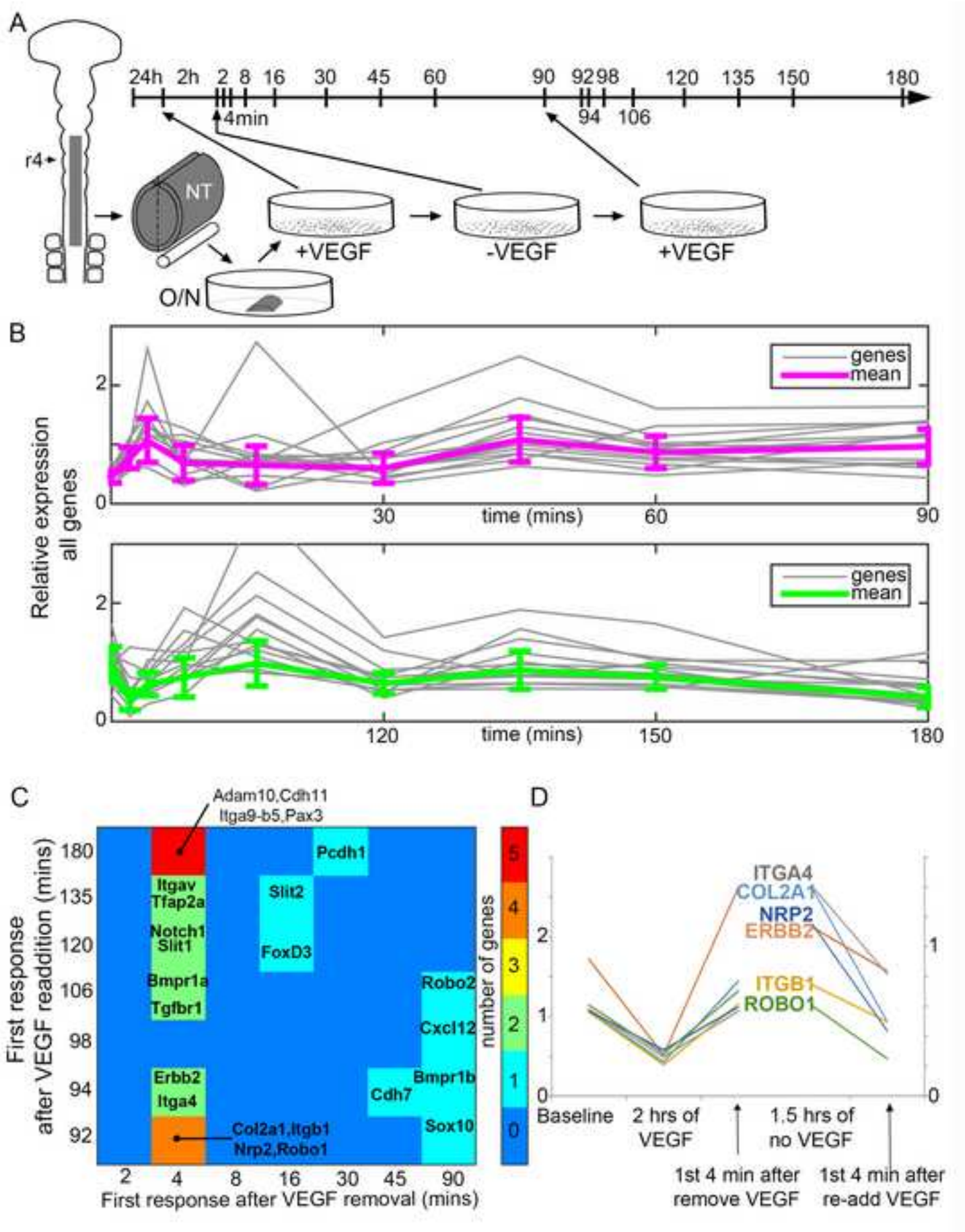

Figure 4

Click here to download high resolution image

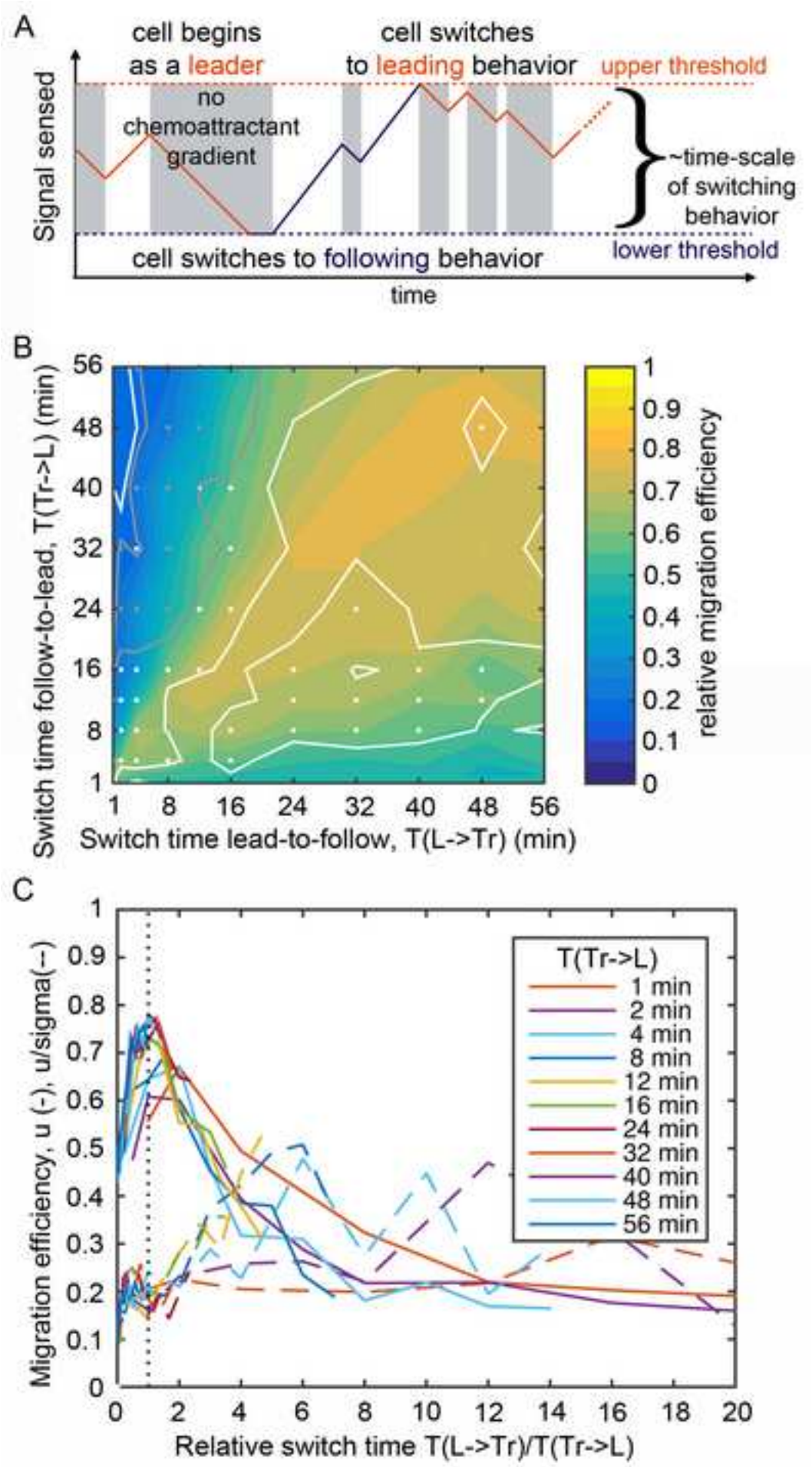

Figure 5

Click here to download high resolution image

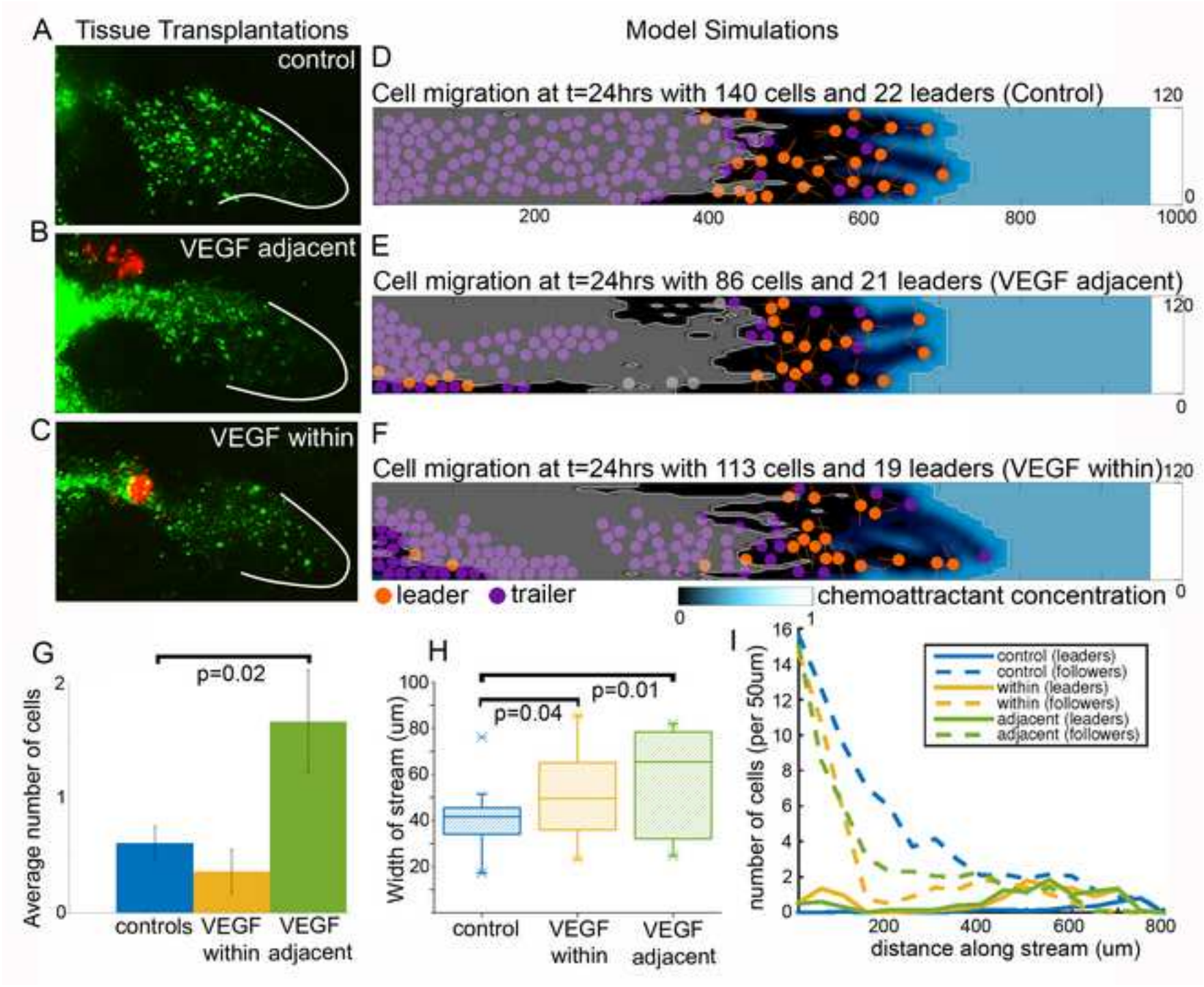

Figure 6

Click here to download high resolution image

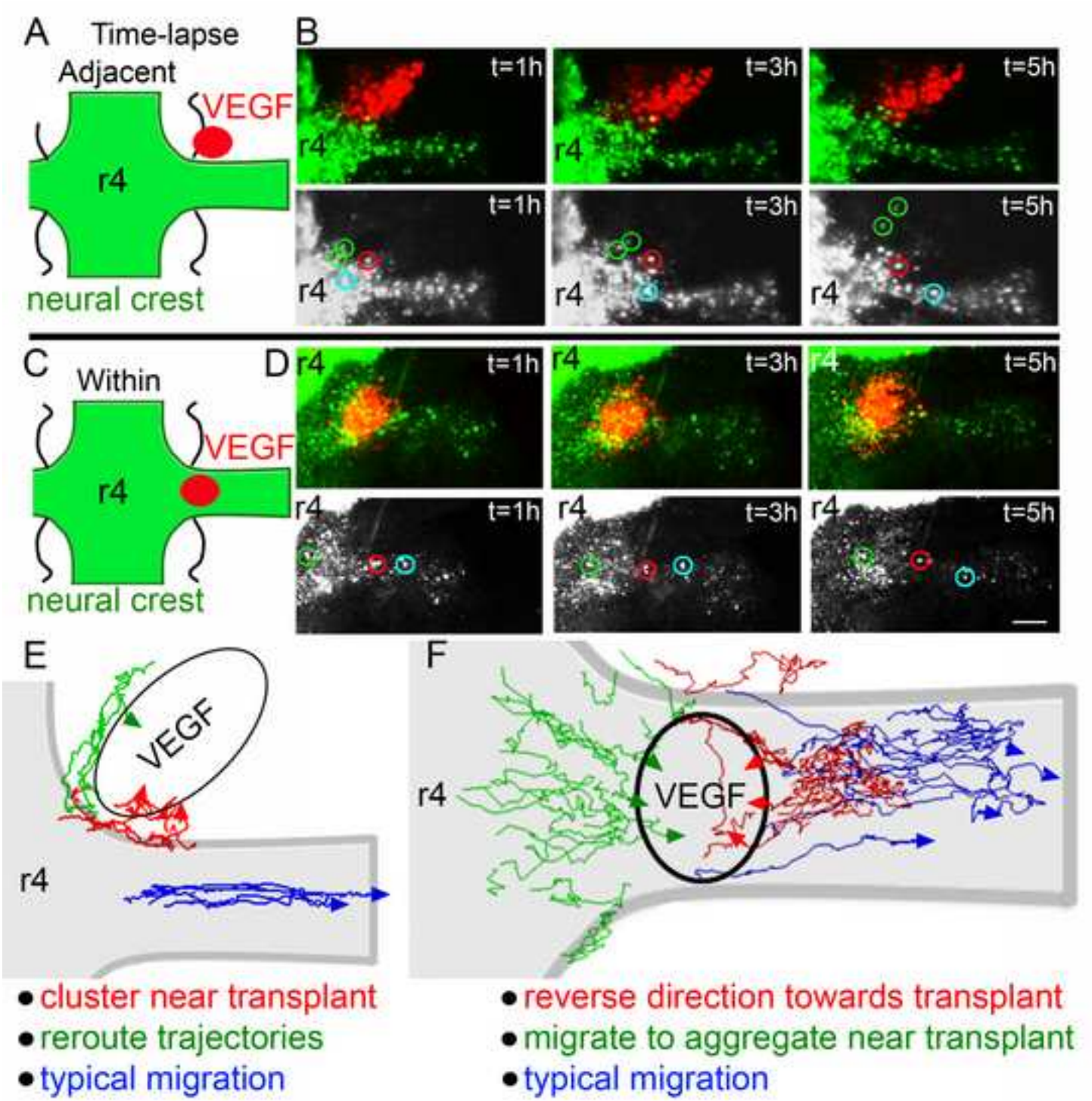

Figure 7

Click here to download high resolution image

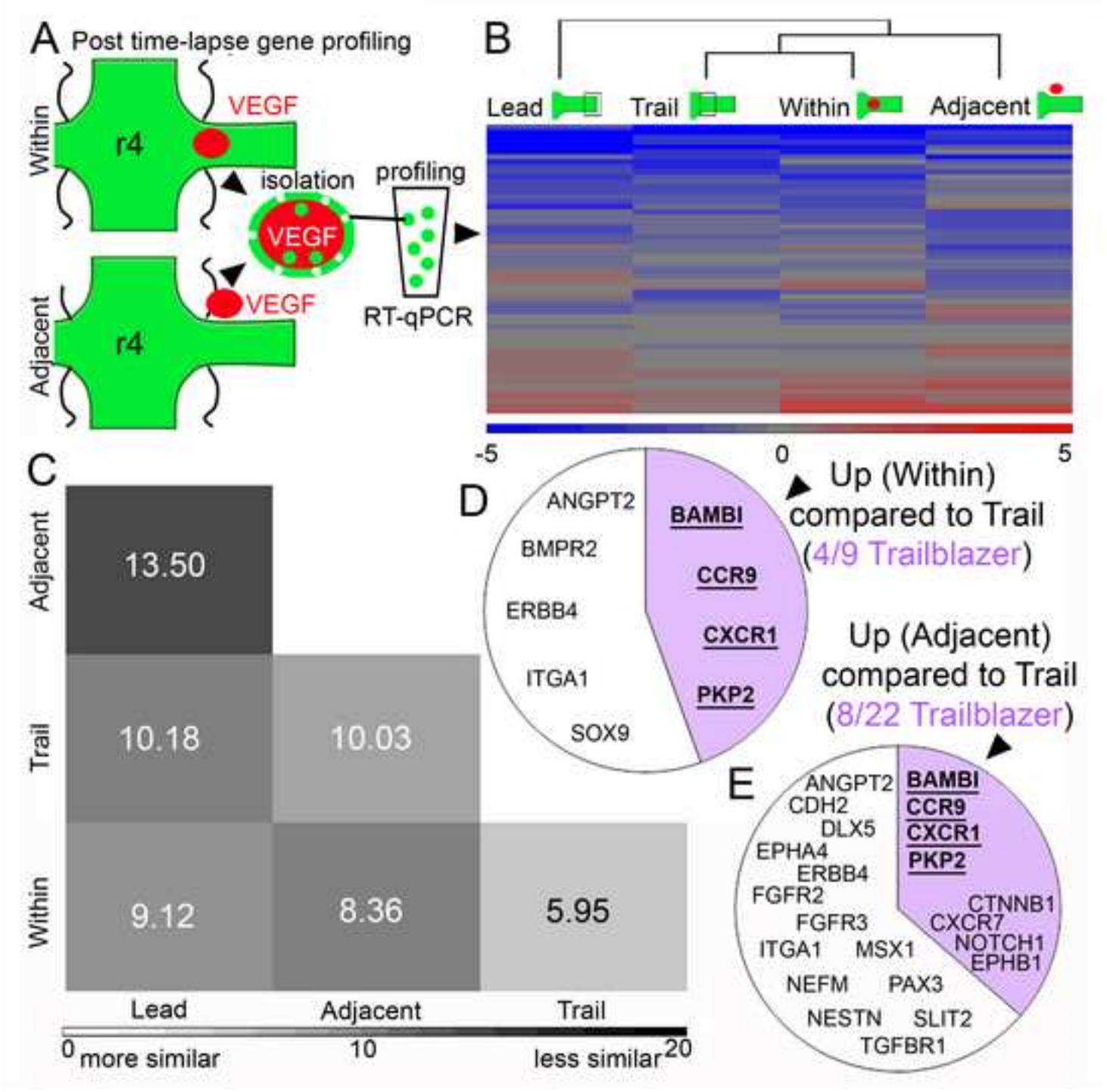

Figure 8

Click here to download high resolution image

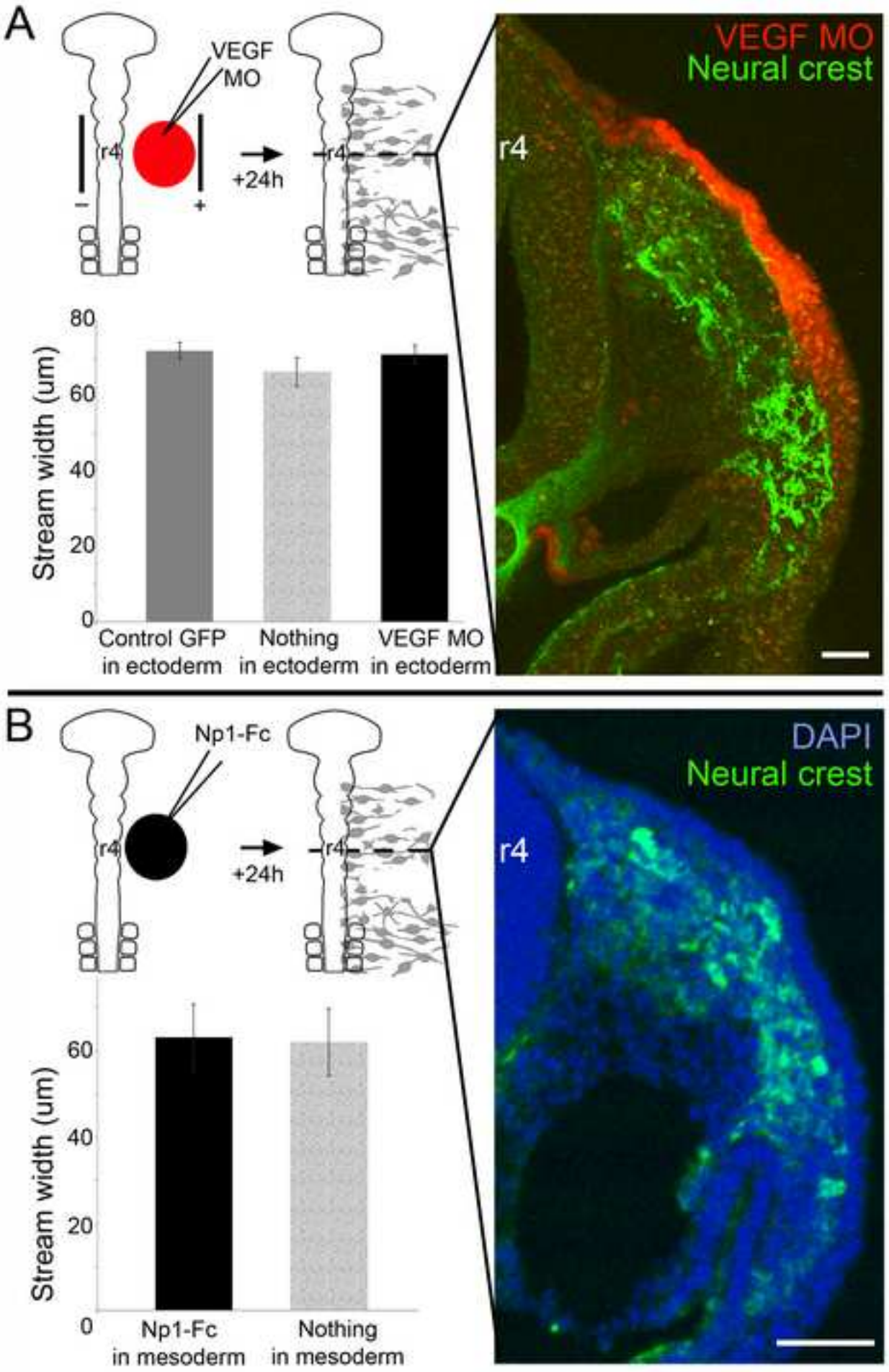

Figure 9

Click here to download high resolution image

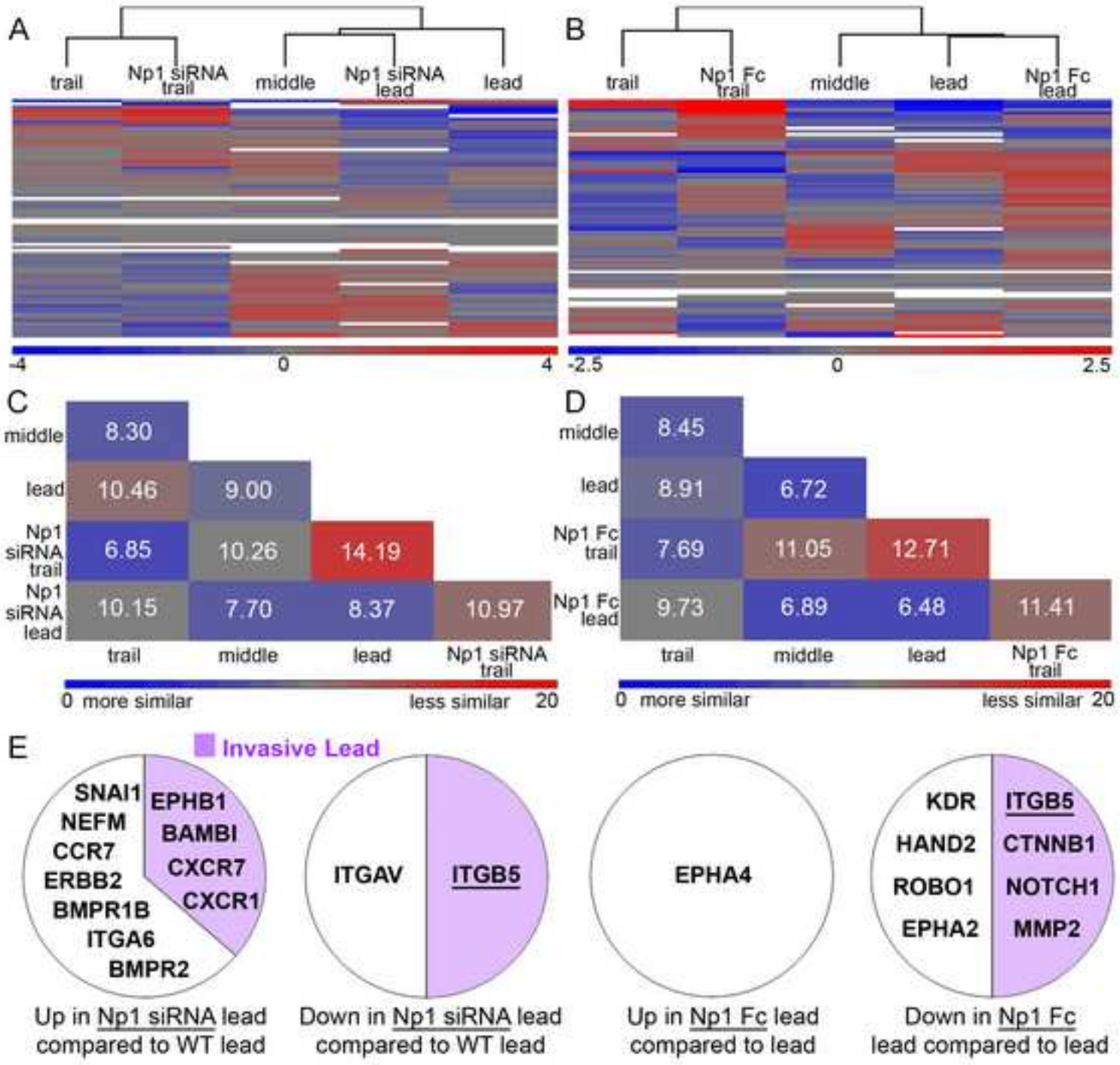

Table 1

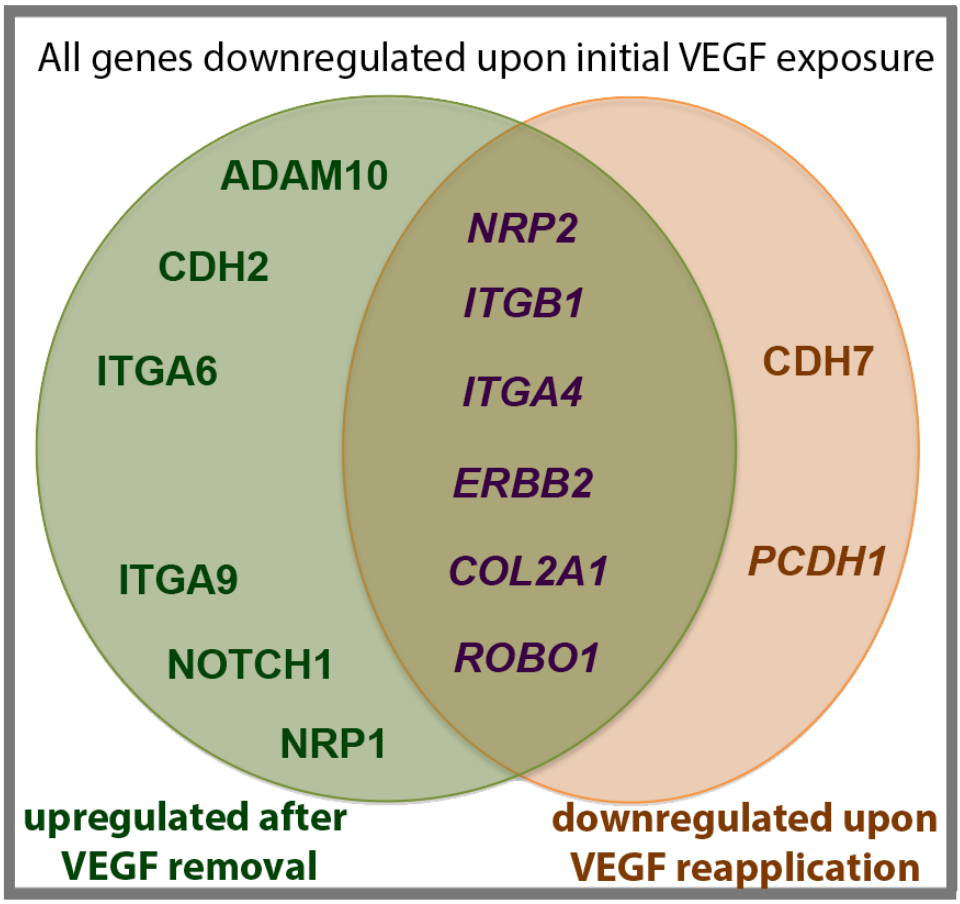

Table 1: Gene expression dynamics within cranial neural crest cells after VEGF exposure, removal, and reapplication in vitro. All genes shown were significantly downregulated upon initial exposure to VEGF. Genes (in green) were significantly upregulated after removal of VEGF, but displayed no significant change upon the reapplication of VEGF. Genes (in orange) displayed no significant change after removal of VEGF, but were significantly downregulated upon the reapplication of VEGF. Genes (in purple and italic) were upregulated after removal of VEGF, and then significantly downregulated upon the reapplication of VEGF.

Table 2: Genes profiled for in vitro versus in vivo experiments

Actb	Pax3
Adam10	Pcdh10
Adam33	Pcdh19
Ankk1	Rplp0
Aqp1	Sfrp1
Bambi	Slit2
Bmpr1a	Snail1
Bmpr1b	Snail2
Ccr9	Sox10
Cdh2	Sox9
Cdh6	Tbp
Cdh7	Tfap2a
Cfc1b	Tgfbr1
Ctnnb1	Unc5b
Cxcr1	Ywhaz
Cxcr4	
Ednra	
Efnb2	
Elav4	
Epha4	
Fgfr1	
Fgfr2	
Foxd3	
Gapdh	
Gpc3	
Hand2	
Hprt	
Isl1	
Itga1	
Itga6	
Itga9	
Itgb1	
Itgb3	
Jag1	
Kdr	
Krt19	
Msx1	
Nefm	
Nestin	
Notch1	
Nrg1	
Nrp1	

Table 3: Genes profiled for timed response to VEGF

Adam10	Gpc3	Spon1
Adam33	Hand2	Tfap2a
Angpt2	Il8	Tgfbr1
Ankk1	Isl1	Th
Aqp1	Itga1	Uncb5
Bambi	Itga4	Vcam
Bmpr1a	Itga6	Wisp1
Bmpr1b	Itga9	Actb
Ccl19	Itgav	Gapdh
Ccr4	Itgb1	Hprt
Ccr5	Itgb5	Rhoa
Ccr7	Kdr	Rplpo
Ccr8	Krt15	Ywhaz
Cdh11	Mbp	Nes
Cdh2	Mitf	Bdnf
Cdh6	Mmp2	Alk
Cdh7	Mmp9	
Cfc1b	Msx1	
Col2a1	Ncam2	
Cxcl12	Nedd9	
Cxcr4	Nefm	
Cxcr5	Notch1	
Dlx5	Nrg1	
Dsp	Nrg2	
Ednra	Nrp1	
Elav4	Nrp2	
Epha1	Pax3	
Epha2	Pcdh1	
Epha3	Pcdh19	
Epha4	Pdgfrl	
Epha6	Perp	
Ephb1	Phox2b	
Ephb3	Pkp2	
Erbb2	Robo1	
Fgf4	Robo2	
Fgf8	Runx2	
Fgfr1	Slit1	
Fgfr2	Slit2	
Fgfr3	Snail1	
Foxd3	Sox10	

Movie 1

Click here to download Supplementary material for online publication only: MOVIE_1_KULESA_ADJACENT.mp4

Movie 2

Click here to download Supplementary material for online publication only: MOVIE_2_KULESA_WITHIN.mp4

Supplementary model information

Click here to download Supplementary material for online publication only: supplementary-model-information 061015.pdf